

Reprint 774

Dual Doppler radar analysis of 3-dimensional
winds for heavy rain events in southern China

P.W. Chan, C.M. Cheng, A.M. Shao* & Y.M. Huang[#]

Fifth European Conference on Radar in Meteorology and
Hydrology, Helsinki, Finland 30 June - 4 July 2008

**Lanzhou University, Lanzhou, China*

*# Air Traffic Management Bureau of Central and Southern Region,
Civil Aviation Administration of China*

Dual Doppler radar analysis of 3-dimensional winds for heavy rain events in southern China

P.W. Chan¹, C.M. Cheng¹, A.M. Shao², and Y.M. Huang³

(1) Hong Kong Observatory, Hong Kong, China, (2) Lanzhou University, Lanzhou, China,

(3) Air Traffic Management Bureau of Central and Southern Region,
Civil Aviation Administration of China

1. Introduction

Southern China is often affected by heavy rain (hourly rainfall of 50 mm or above) in late spring and in summer every year. The deluge is usually associated with a trough of low pressure, active southwest monsoon or tropical cyclones. Detailed study of the kinematic structures of the heavy rain would help the monitoring and prediction of the rainstorms.

Doppler weather radars are widely used in southern China for heavy rain monitoring and nowcasting. This paper uses the data from two radars, namely, one in Hong Kong and another in Guangzhou, to analyze the 3D wind fields in two heavy rain episodes in summer 2007. The wind field is obtained from the radial velocity and the reflectivity data by a variational method. The technical information of the two radars is briefly summarized in Section 2. The 3D wind field analysis method is described in Section 3. Two case studies are presented in Section 4, and the conclusions are drawn in Section 5.

2. Radars in the study

The two radars used in this study are the Hong Kong radar at Tate's Cairn and Guangzhou radar near the Beiyun International Airport (locations given in Figure 1(a)). Both of them are Doppler weather radars.

The Hong Kong radar (22°21'36''N 114°12'54''E) is an S-band radar located at around 585 m AMSL on top of a hill. It scans at 12 different elevation angles from 0.5° to 34.7°. The volume scan takes about 6 minutes to complete. The Nyquist velocity is 44.4 m/s for elevation angles between 0.5° and 6.7°, and 48 m/s for elevation angles between 9.1° and 34.7°.

The Guangzhou radar (23°24'18''N 113°15'30''E) is a C-band radar located at around 56 m AMSL. It scans at 10 different elevation angles from 0.3° to 33°. The volume scan takes about 10 minutes to complete. The Nyquist velocity is 26.7 m/s

3. 3D wind field analysis method

Before the analysis, the radar data are interpolated into a Cartesian grid. The grid has 250 x250 points with a grid size of 800 m. In the vertical, the radar data extend from the ground up to 10 km with a resolution of 500 m.

A two-step variational method as described in [1] is employed here to analyze the radial velocity data from the two radars. This method has been used in the dual Doppler

analysis of a LIDAR and a radar at an airport [2]. Only a summary of the method is given here. The retrieval process involves the minimization of a cost function in the following form:

$$J(u, v, w) = J_B + J_{r1} + J_{r2} + J_E + J_C + J_P \quad (1)$$

where (u, v, w) is the 3D wind field to be retrieved.

Each term in (1) is discussed below. J_B is related to the background wind field, given by:

$$J_B = \frac{1}{2} \sum_{i,j,k} [W_{uB} (u - u_B)^2 + W_{vB} (v - v_B)^2 + W_{wB} (w - w_B)^2] \quad (2)$$

where the W 's are the weighing factors and the subscripts B refer to the background wind field obtained by minimizing (1) without considering the J_B term in (2), i.e. setting the weights $W_{uB}=W_{vB}=W_{wB}=0$.

J_{rm} ($m=1$ and 2 , the index of the radar) is related to the convergence of the retrieved radial velocities (i.e. component of the retrieved wind vector along the direction of the measurement radial of the radar) to the observed radial velocities from the two radars. It is given by:

$$J_{rm} = \frac{1}{2} \sum_{i,j,k} W_{rm} (v_{rm} - v_{rm}^{obs})^2. \quad (3)$$

In determining the retrieved radial velocity, the fall velocity W_T of rain drop is included:

$$v_{rm} = \frac{(x - x_m)u + (y - y_m)v + (z - z_m)(w - w_T)}{\sqrt{(x - x_m)^2 + (y - y_m)^2 + (z - z_m)^2}}$$

where (x, y, z) is the grid point, (x_m, y_m, z_m) is the location of the radar, and (u, v, w) is the retrieved velocity. The fall velocity is based on an empirical relationship with the reflectivity of the radar echo [1].

J_E is the constraint related to conservation of reflectivity:

$$J_E = \frac{1}{2} \sum_{i,j,k} W_E E^2 \quad (4)$$

where E is calculated from

$$E = \frac{\partial \eta}{\partial t} + u \frac{\partial \eta}{\partial x} + v \frac{\partial \eta}{\partial y} + w \frac{\partial \eta}{\partial z}$$

and η is the reflectivity of the radar echo.

J_c is the constraint based on continuity equation:

$$J_c = \frac{1}{2} \sum_{i,j,k} W_c \left(\frac{\partial u}{\partial x} + \frac{\partial v}{\partial y} + \frac{\partial w}{\partial z} - kw \right)^2, \quad (5)$$

where $k = -\partial(\ln \rho_0) / \partial z$.

Finally, J_p is the smoothing term:

$$J_p = \frac{1}{2} \sum_{i,j,k} [W_{up} (\nabla^2 u)^2 + W_{vp} (\nabla^2 v)^2 + W_{wp} (\nabla^2 w)^2] \quad (6)$$

where ∇^2 is the Laplacian operator.

The values of the various weighing factors are: $W_{uB}=W_{vB}=W_{wB}=1.0$, $W_{rm}=1.0$, $W_E=0.01d^2$, $W_C=100d^2$, $W_{up}=W_{vp}=1.0d^2$, and $W_{wp}=0.25 W_{up}$, in which d is the horizontal grid size.

4. Case studies

Two heavy rain cases in summer 2007 are considered here. The first one occurred in the morning of 24 April 2007. Synoptically, an E-W oriented trough of low pressure affected southern China and moved southwards across the coastal areas. Figure 1(a) shows the analyzed horizontal wind vectors at 1 km AMSL at 01 UTC (9 a.m., with Hong Kong time = UTC + 8 hours) on that day when the heavy rain was located between Hong Kong and Guangzhou. Strong northwesterly winds (30 knots or above) appeared over and to the north of the rain cells in the inland areas (the rain cells are depicted in the reflectivity plot in Figure 2(a)), and they converged with the moderate southwesterly winds ahead (to the south) of the rain cells. Speed convergence of north to northwesterly winds was also evident at about 20 km to the north of Hong Kong. These convergent flow areas showed up nicely in the convergence field (negative divergence) in Figure 1(b).

In the middle troposphere (3 km AMSL), southwesterly to northwesterly flow appeared over the inland areas, and they converged with the south to southeasterly flow along the coast at the frontier part of the rain cells (Figure 1(c)). Upward motion could be analyzed at location of airflow convergence (Figure 1(d)). Such upward motion did not just happen in the middle troposphere, but extended to higher altitude as well. For instance, at 8 km AMSL, a jet of 50 knots appeared to the northwest of Hong Kong over the inland areas (Figure 1(e)), and it was associated with a board area of upward motion (Figure 1(f)).

Vertical cross sections are made across the rain cells to understand the vertical circulations associated with the heavy rain. In the cross-section AB (location in Figure 2(a)), upward motion is generally found at the locations of the intense rain cells (Figure 2(b)), though the magnitude (maximum of 4.5 m/s) seems to be a bit smaller

considering the rather intense convection. Nearly zero vertical velocity or even downward motion is generally analyzed in between the intense rain cells. Across the rain cell (cross section CD in Figure 2(a)), rear inflow appeared in the first few km above ground behind the intense rain cell. A vertical circulation also occurred inside the cell, with vertical motion (up to 4 m/s) at the frontier and downward motion (up to 3 m/s) just behind. These flow features are generally consistent with those found in a squall line.

The second case occurred on 19 May 2007. An E-W lying trough of low pressure over the northern part of South China Sea brought unsettled weather to southern China. Figure 3(a) shows the analyzed horizontal wind field at 1 km AMSL when the rain cells (locations given in Figure 3(d)) affected the coastal areas including Hong Kong. Cyclonic flow could be analyzed at these locations of intense convection with a northwesterly jet of 25 knots behind the convection (i.e. to the northwest).

In the middle troposphere (4 km AMSL), a southwesterly jet of 40 knots appeared over the inland areas, whereas only a moderate to fresh southwesterly airstream prevailed along the coast (Figure 3(b)). Upward motion could be analyzed in association with the jet and in the coastal area (Figure 3(c)). A vertical cross section AB is made across the rain cells (Figure 3(d)). Upward motion could be analyzed at the locations of the rain cells, though the magnitude was rather small (a couple of m/s only, Figure 3(e)). On the other hand, more significant upward motion (4 m/s) is found at the low-level cyclone over Hong Kong (Figure 3(a)).

5. Conclusions

The radial velocity and reflectivity data from two Doppler weather radars at southern China are used to analyze the kinematic structures of heavy rain in the region. A two-step variational method is adopted to analyze the 3D wind field. The results of two case studies are presented here. The 3D wind fields depict many interesting features about the rain events. Within the boundary layer, convergent flow or cyclonic flow could be analyzed at the locations of the rain cells. Jets and upward motion are found in the middle or even the upper troposphere. Vertical cross sections are made across the rain cells. In one case (24 April 2007), some flow features typically found in squall lines show up in the cross section, such as rear inflow in the lower to middle troposphere, and vertical circulation within the rain cell. The variational method discussed in the paper appears to be robust in depicting the major features of the airflow in heavy rain. Its operational application to the radar data would be studied further.

References

- [1] Y. Yang and C.J. Qiu, "Analysis on mesoscale circulation within a heavy rain system using Doppler radar data", Plateau Meteorology, Volume 25, pp. 925-931 (in Chinese with English abstract), 2006.
- [2] P.W. Chan and A.M. Shao, "Depiction of complex airflow near Hong Kong International Airport using a Doppler LIDAR with a two-dimensional wind retrieval technique", Meteorologische Zeitschrift, Volume 16, Number 5, pp 491-504, 2008.

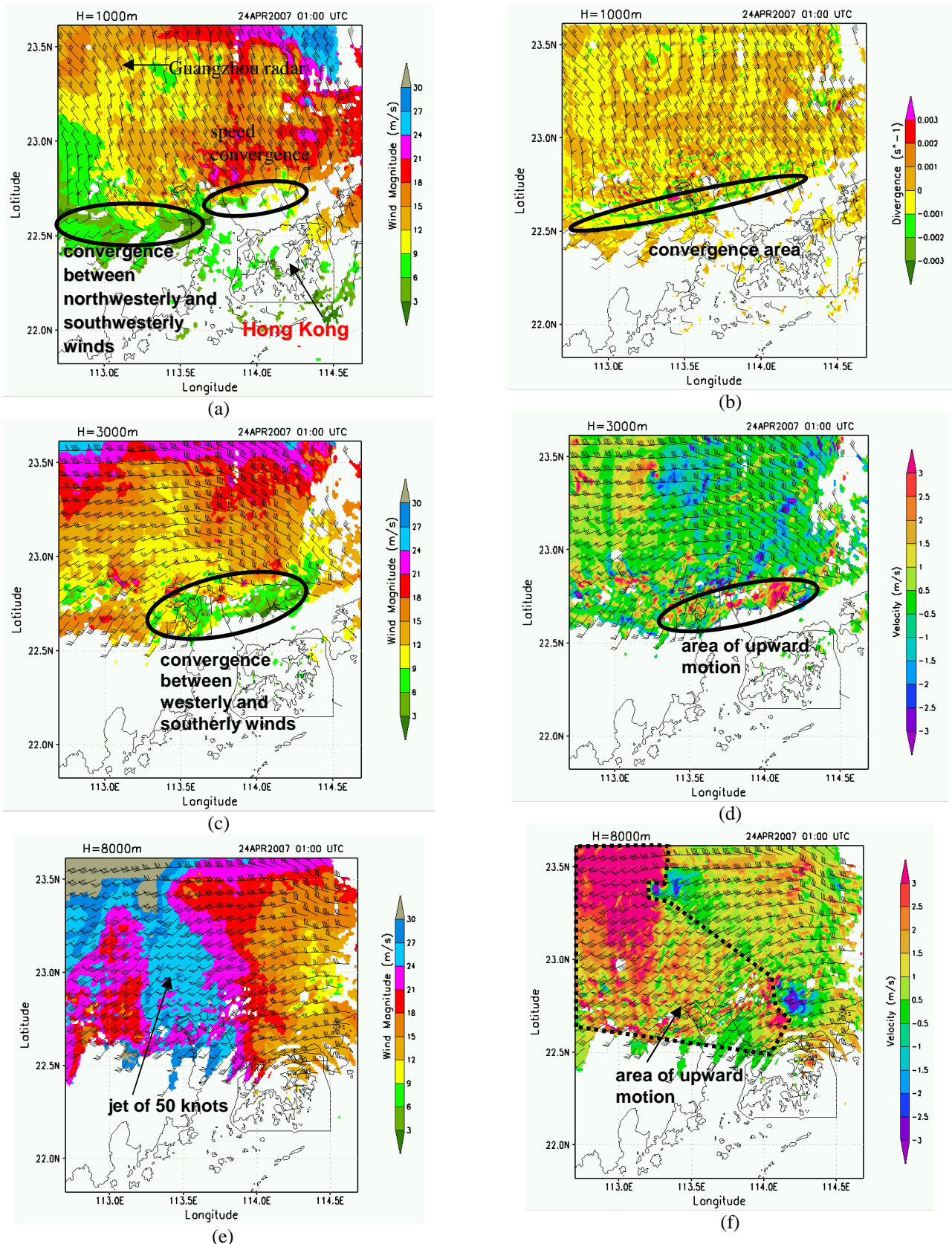


Fig. 1 (a) shows the analyzed horizontal wind vectors at 1 km AMSL, with the colour contours showing the magnitude of the wind vector. (b) is the divergence field for the wind vectors in (a). (c) shows the horizontal wind vectors at 3 km AMSL. (d) is the vertical velocity field at this height. (e) shows the horizontal wind vectors at 8 km AMSL, and (f) is the vertical velocity field at this height.

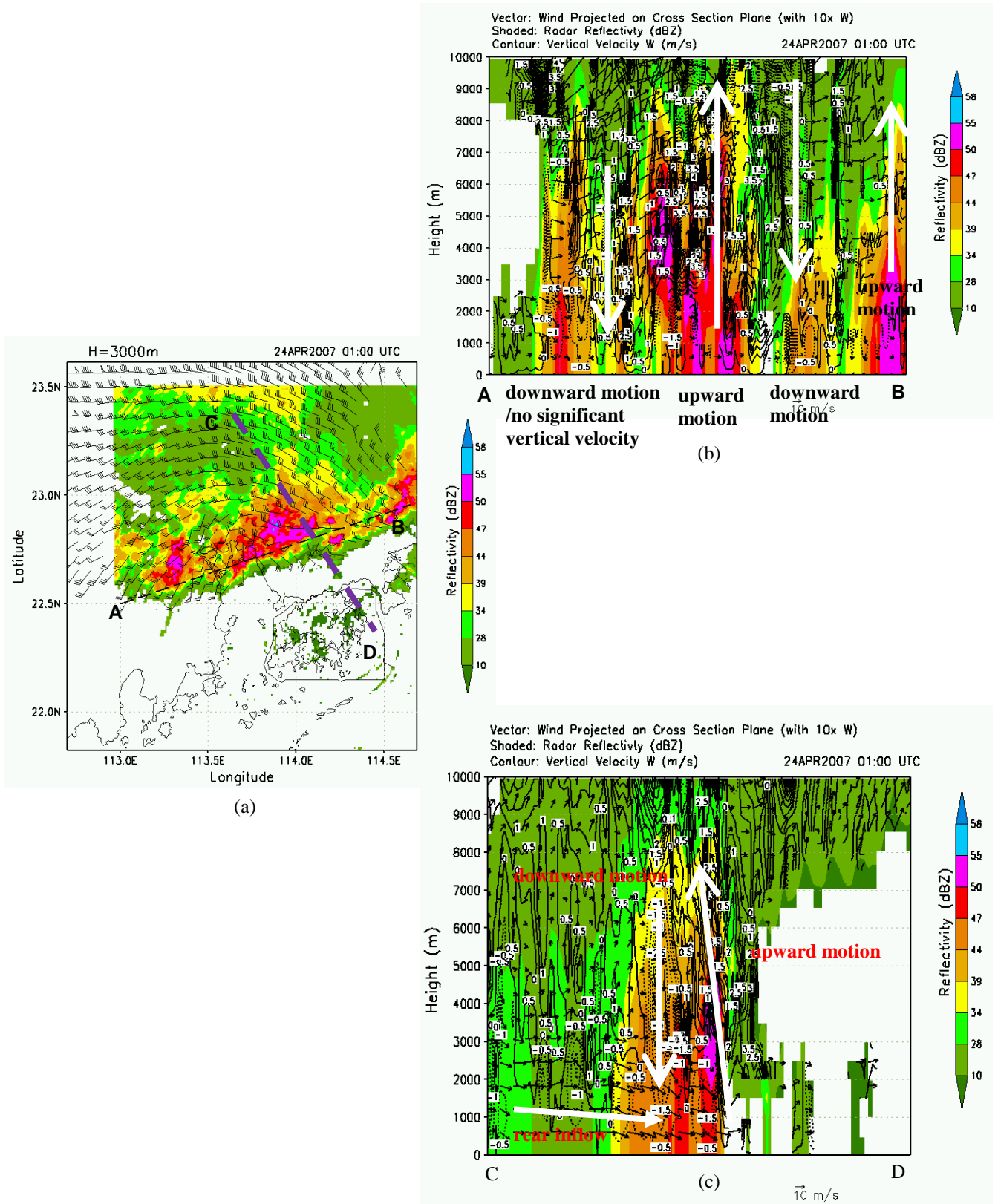


Fig. 2 (a) shows the radar reflectivity of Hong Kong radar at 3 km AMSL (only those used in the present analysis of 3D wind field is depicted) and the locations of the vertical cross sections AB and CD. (b) is the vertical cross section AB, showing the radar reflectivity and the analyzed wind field (projected on the vertical cross sectional plane, with the vertical velocity multiplied by 10). (c) is the corresponding figure for vertical cross section CD. The rain cells were moving from C to D.

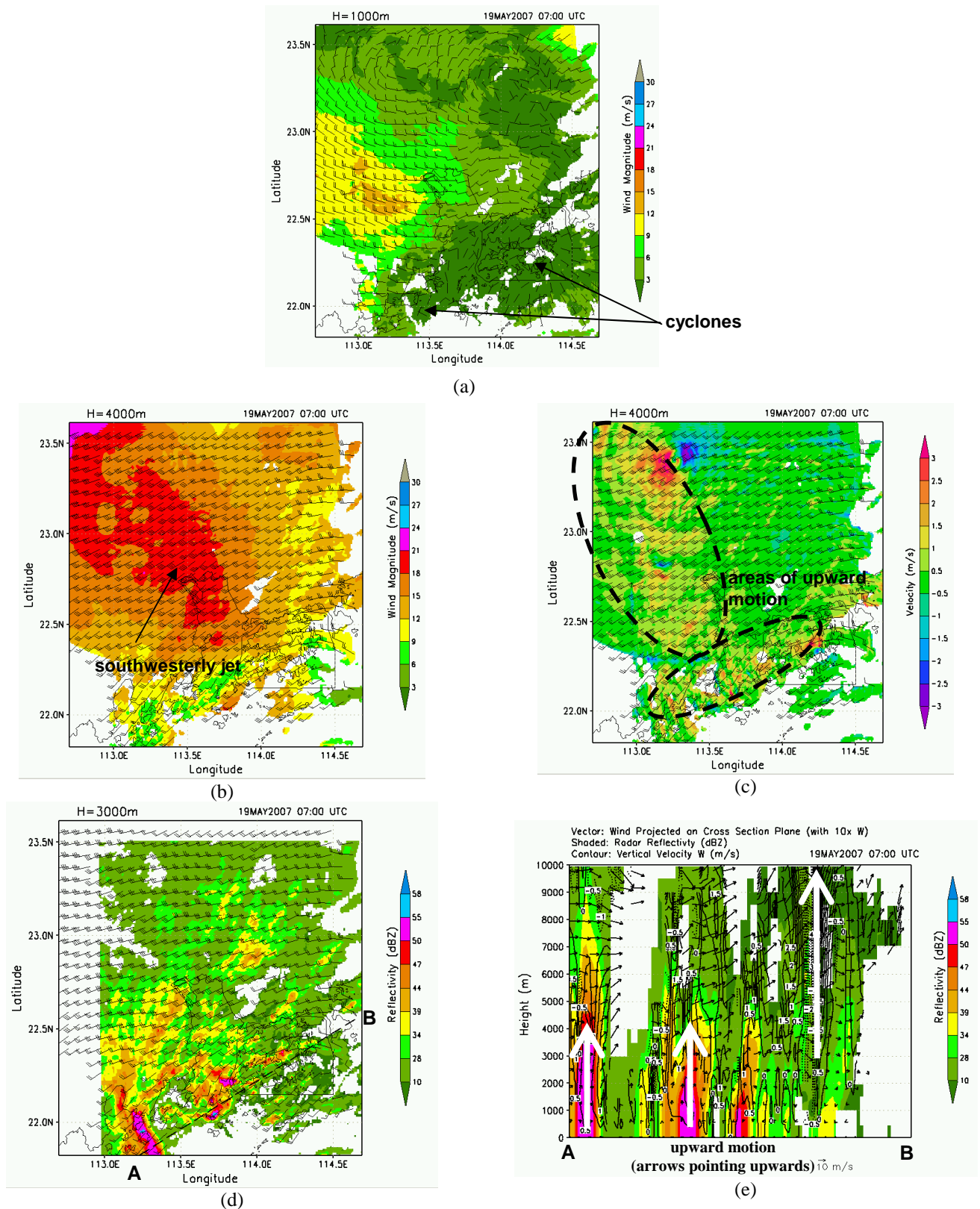


Fig. 3 (a) shows the analyzed horizontal wind field at 1 km AMSL, with the colour contours giving the magnitude of the wind vector. (b) shows the wind field at 4 km AMSL, and (c) is the corresponding vertical velocity field. (d) shows the radar reflectivity of Hong Kong radar at 4 km (only those used in the present 3D wind field analysis is depicted) with the location of vertical cross section AB. (e) gives the radar reflectivity and the wind field projected on the cross sectional plane AB (vertical velocity multiplied by 10).